MARS SCIENCE LABORATORY INTERPLANETARY NAVIGATON ANALYSIS

Tomas J. Martin-Mur (1), **Gerard L. Kruizinga** (2), **Mau C. Wong** (3),
Jet Propulsion Laboratory, California Institute of Technology,
4800 Oak Grove Drive, Pasadena, CA 91109, USA,
(1)+1-818-393-6276, Tomas.J.Martinmur@jpl.nasa.gov
(2)+1-818-354-7060, Gerhard.L.Kruizinga@jpl.nasa.gov
(3)+1-818-354-7405, Mau.C.Wong@jpl.nasa.gov

Abstract: The Mars Science Laboratory (MSL) is a NASA rover mission that will be launched in late 2011 and will land on Mars in August of 2012. This paper describes the analyses performed to validate the navigation system for launch, interplanetary cruise, and approach. MSL will use guidance during its descent into Mars in order to minimize landing dispersions, and therefore will be able to use smaller landing zones that are closer to terrain of high scientific interest. This will require a more accurate delivery of the spacecraft to the atmospheric entry interface, and a late update of the state of the spacecraft at entry. During cruise and approach the spacecraft may perform up to six trajectory correction maneuvers (TCMs), to target to the desired landing site with the required flight path angle at entry. Approach orbit determination covariance analyses have been performed to evaluate the accuracy that can be achieved in delivering the spacecraft to the entry interface point, and to determine how accurately the state of the spacecraft can be predicted to initialize the guidance algorithm. In addition, a sensitivity analysis has been performed to evaluate which factors most contribute to the improvement or degradation of the navigation performance, for both entry flight path angle delivery and entry state knowledge.

Keywords: Mars, navigation, orbit determination, covariance analysis

1. Introduction

The Mars Science Laboratory (MSL) is a NASA rover mission that will be launched in late 2011 and will land on Mars in August of 2012. The MSL rover will carry the largest and most advanced suite of scientific instruments ever landed on the Martian surface, and it will be accurately delivered to the surface by an innovative system for descent and landing, to a site of high scientific interest that could not be reached without using guidance during the hypersonic flight phase in the Mars atmosphere.

In order to use the guidance system two main actions are necessary from the navigation system. The first is that the spacecraft needs to be delivered with high accuracy to atmospheric entry interface point at Mars. The second is that the position and velocity of the spacecraft at entry, relative to Mars, needs to be known with high accuracy, in order to initialize the guidance system. The guidance system modulates the bank angle of the entry vehicle in order to use lift to adjust its heading and manage altitude change. Errors in the inputs, models, sensors, and actuators used by the guidance system increase the size of the delivery footprint. The initialization of the state of the spacecraft, both in position and velocity, and in orientation, is fundamental to reduce the propagation of errors and to be able to accurately target the desired landing point. High delivery accuracy is required in order to reduce the range of possible conditions over which the guidance system has to work, increasing the safety margins against anomalies or unexpected environmental conditions.

The MSL navigation system consists of three main functional elements: spacecraft trajectory propagation and analysis, spacecraft trajectory determination, and propulsive maneuver design and analysis. The primary navigation functions during MSL flight operations are the following:

- Process radiometric tracking data – Doppler, range, and doubly-differenced one-way range (ΔDOR) – to estimate the spacecraft trajectory and associated uncertainties.

- Perform Entry, Descent and Landing (EDL) trajectory analysis to determine desired atmospheric entry aimpoints for Trajectory Correction Maneuvers (TCMs) and to evaluate landing site coordinates and landing footprints.

- Determine the desired delta velocity (ΔV) vector for TCMs to achieve the specified atmospheric entry aimpoint and verify the TCM implementation provided by spacecraft team.

- Generate the spacecraft ephemeris and ancillary trajectory data products.

- Provide real-time monitoring during TCMs and reconstruct the TCM ΔV using pre- and post-TCM tracking data.

- Perform EDL trajectory analysis to provide inputs for uplink of EDL parameter updates, including an estimate of the atmospheric entry state vector for initializing the hypersonic entry guidance algorithm.

- Provide support for the UHF communications links between the rover and the Mars Odyssey and MRO orbiters.

2. The Mars Science Laboratory Mission

The Mars Science Laboratory will be delivered to one of four candidate landing sites on the surface of Mars [1]. These landing sites are of high scientific interest and have been deemed safe for landing by the MSL project. The landing sites were selected taking into account their scientific merit and engineering constraints. The final landing site is schedule to be selected after completion of the fifth and final MSL Landing Site Workshop in April of 2011, and the EDL Landing Site Safety Review in May 2011. Table 1 shows the areocentric coordinates and characteristics of the candidate landing sites and Figure 1 shows the location of possible landing ellipses on the surface of Mars.

Table 1. Characteristics of the MSL Candidate Landing Sites

Landing Site	Latitude (deg)	East Longitude (deg)	MOLA elevation (Km)	Main Characteristics
Mawrth Vallis	23.99 N	341.04	-2.2	Extremely ancient section of rocks from the Noachian epoch of early Mars
Gale Crater	4.49 S	137.42	-4.4	The thickest and most diverse exposed stratigraphic section accessible in Mars
Eberswalde Crater	23.90 S	326.74	-1.4	A drainage area with well defined and exposed deposits
Holden Crater Fan	26.40 S	325.16	-2.2	Alluvial fans, stratographic sections, flood deposits, bedrock outcrops

The MSL rover, named Curiosity, will be approximately twice as long and four times as heavy as the Mars Exploration Rovers (MER) launched in 2003, and will carry a payload 10 times heavier than that of those rovers [3]. Figure 2 shows an artist conception of the rover on the surface of Mars. Curiosity carries equipment to gather samples of rocks and soil, crush them, and distribute them to onboard test chambers, as well as a laser that can pulverize materials up to 10 meters away to perform spectral analysis to determine their composition. The rover will be able to travel up to 200 meters per day and will carry a radioisotope power system to recharge its batteries, so they can be used to drive the rover and to power the rover instruments and subsystems.
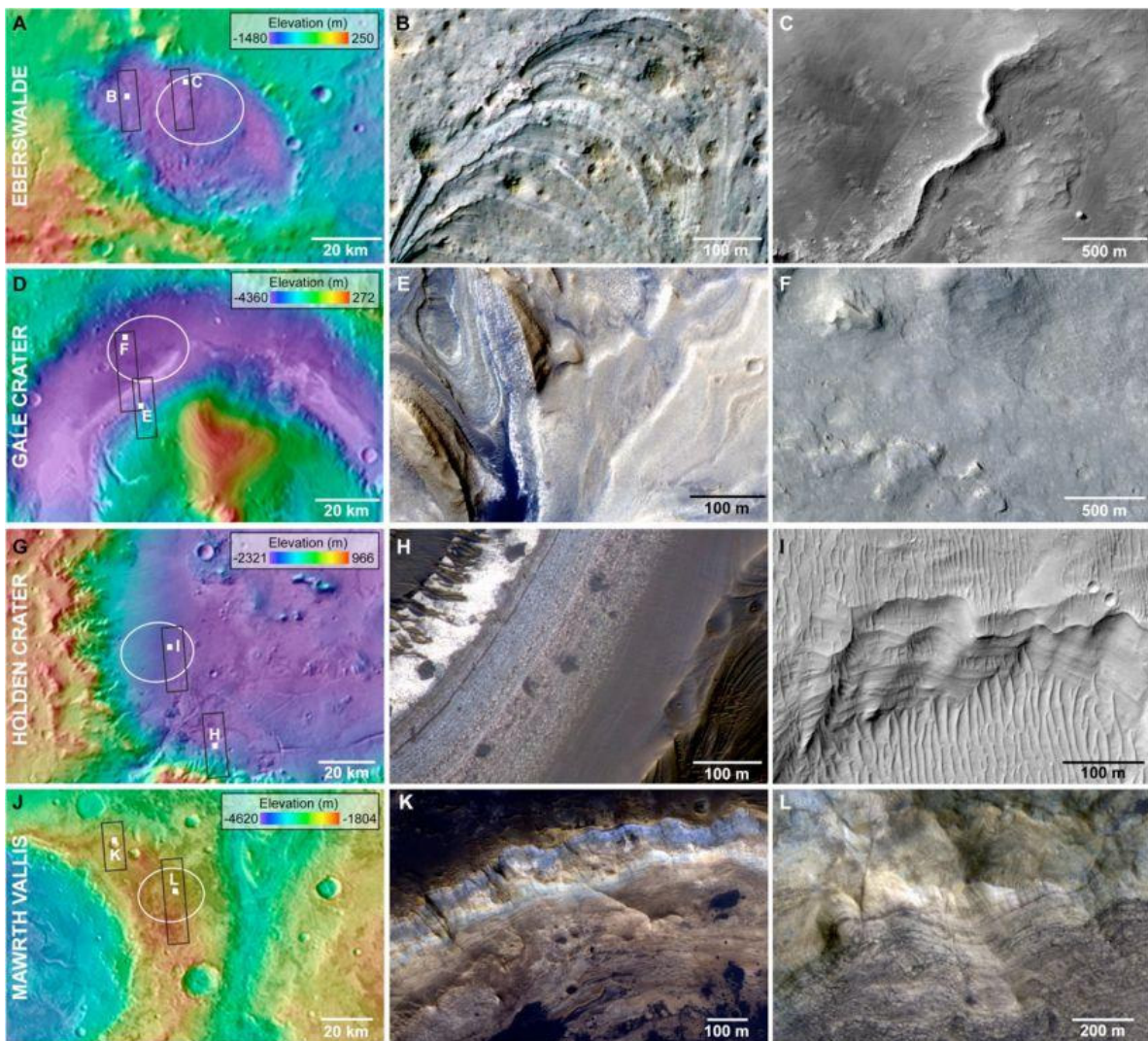
Figure 1. The MSL Candidate Landing Sites [2]

Figure 2. Artist Conception of the MSL Rover on the Surface of Mars

The MSL spacecraft (Fig. 3) will be launched on a United Launch Alliance (ULA) Atlas V 541 launch vehicle from Cape Canaveral Air Force Station Space Launch Complex 41, during one of three launch/arrival sets, all based on a Type I transfer trajectory to Mars. The first set, named Type 1A, has a launch period duration of 24 days extending from November 25, 2011 through December 18, 2011, with arrival dates on Mars between August 6, 2012 and August 20, 2012. The second set, Type 1B, also has a launch period duration of 24 days extending from November 25, 2011 through December 18, 2011, with a constant arrival date of August 6, 2012. The third set, Type 1C, has a duration of 20 days extending from November 29, 2011 through December 18, 2011, with arrival dates on Mars between August 8, 2012 and August 13, 2012. The launch/arrival sets are limited by the performance of the launch vehicle and the desired entry velocity at Mars. The three launch/arrival sets offer alternative ways of performing communication during EDL, in order to monitor the performance of the vehicle during this highly critical mission phase. EDL communication will be accomplished via an UHF relay link through the Mars Reconnaissance Orbiter, the Mars Odyssey orbiter, and the ESA Mars Express orbiter, and through an X-band direct-to-earth (DTE) link, when available. The ascending node of the NASA orbiters and the orbital phasing of all three orbiters may need to be adjusted in order to ensure that they can track MSL during EDL. DTE visibility is dependent on the date of arrival and the latitude of the landing site, as in some cases the spacecraft is occulted by Mars during its final descent to the surface of the planet. During interplanetary Cruise, the spacecraft will spin around the Z axis at approximately two revolutions per minute.
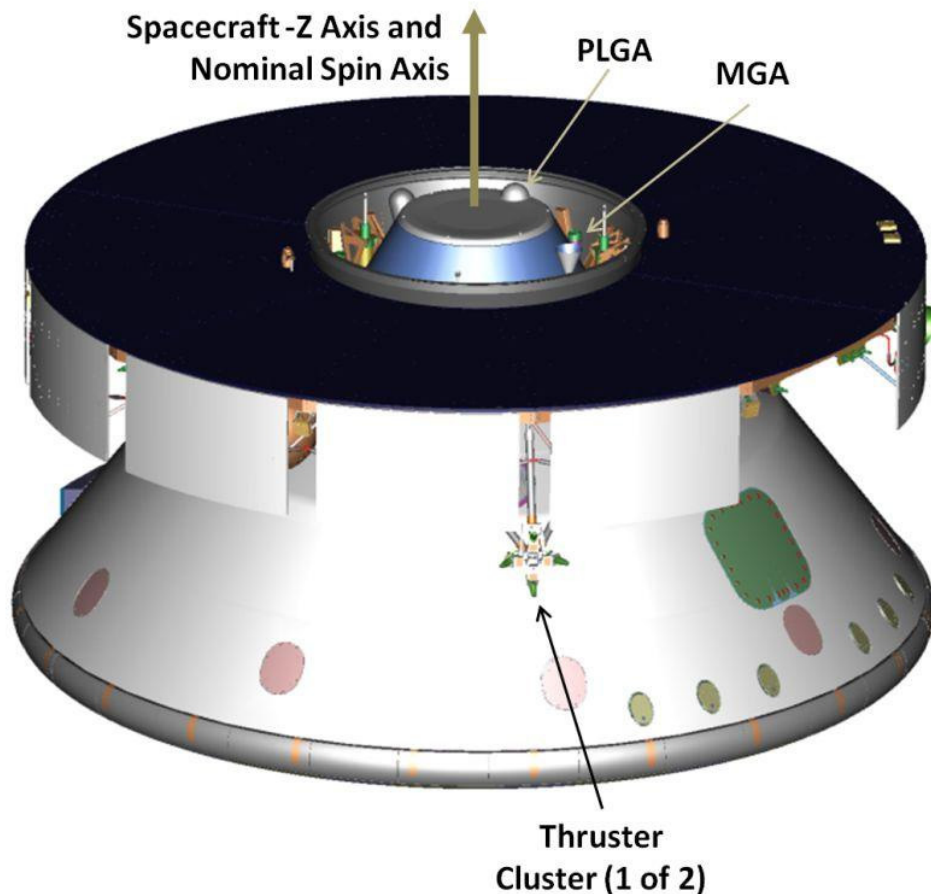

Figure 3. The MSL Spacecraft Cruise Configuration

During the approximately eight-month interplanetary transfer, which includes the Cruise and Approach mission phases, up to six TCMs will be performed to deliver the flight system to the

specified Mars atmospheric entry aimpoint. In addition, during the Cruise phase, instrument checkouts and a characterization of the performance of the Attitude Control, System (ACS) will be performed. The EDL phase begins at the atmospheric entry interface point, which is defined to be at a Mars radius of 3522.2 km. Communications during the interplanetary phase are accomplished via the Parachute cone Low Gain Antenna (PLGA) and a Medium Gain Antenna (MGA), using an X band link.
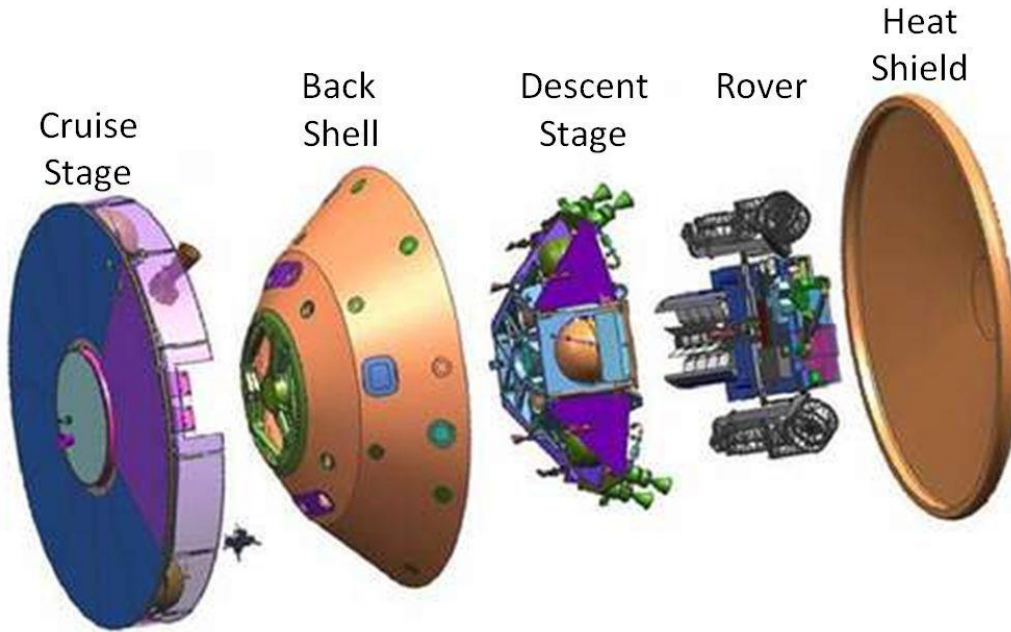

Figure 4. The MSL Flight System Elements

The MSL flight system (Fig.4) consists of four major elements: cruise stage, aero shell (heat shield and back shell), descent stage, and rover. The aero shell encloses the descent stage and rover.
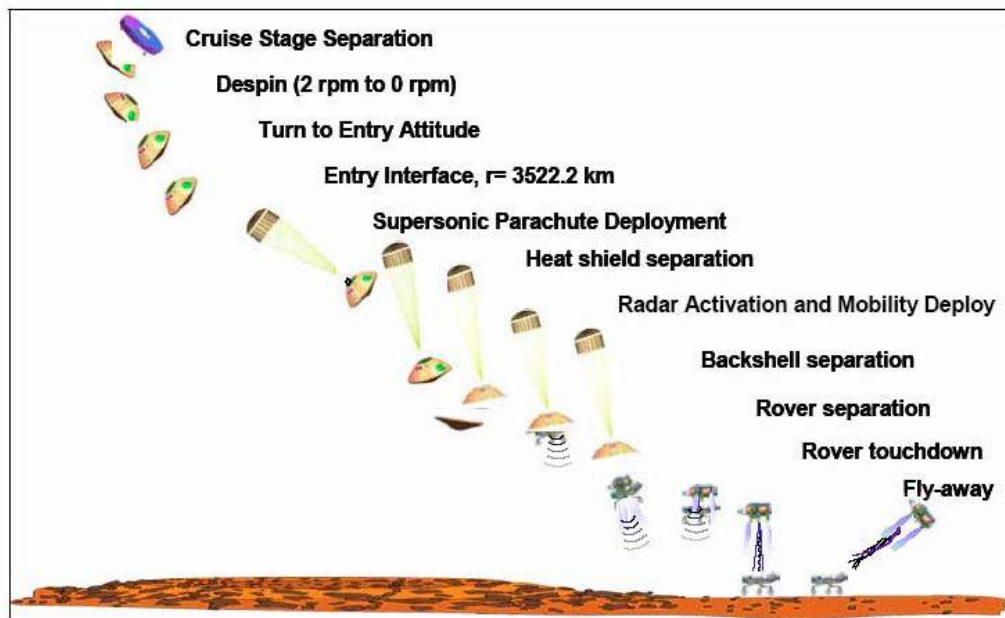

Figure 5. EDL Sequence of Events

The EDL system (Fig. 5) builds upon the heritage of the Mars Pathfinder (MPF) and MER missions, both of which employed an airbag landing system, while adding several major design changes: namely, a lifting aero shell, hypersonic entry guidance, and powered descent. These changes are required to land a rover of much higher mass than either MPF or MER. During the guided hypersonic entry period, the entry vehicle performs a series of roll maneuvers to modulate the aerodynamic lift vector in order to fly out atmospheric entry delivery errors and counteract aerodynamic and atmospheric dispersions, thereby minimizing landing dispersions. A parachute is deployed to reduce speed, and shortly thereafter, the heat shield is jettisoned, exposing the descent stage and attached rover. At the appropriate time, the descent stage engines ignite, and the back shell and parachute will separate. The descent stage engines are used to further reduce speed to nearly zero. Approximately 19 meters above the surface, the descent stage begins to lower the rover, whose wheels have been deployed during the descent, to the surface utilizing a sky crane mechanism. After the rover touches down on the surface, the descent stage releases the rover, executes a divert maneuver to distance itself from the rover, and eventually impacts the surface a safe distance from the rover.

3. Launch and Early Acquisition

Launch navigation's primary task is to provide spacecraft trajectories that satisfy the pointing and frequency generation requirements for Deep Space Network (DSN) initial acquisition and two-way communication in the first few hours after launch. The pointing and frequency predicts for the very first DSN station to acquire the spacecraft signal after launch will be based on pre-launch nominal trajectories, selected based on the actual launch time. However, due to injection errors, the trajectory may need to be updated for generating acquisition predicts at subsequent stations.

For MSL, DSN initial acquisition after launch always occurs at the Canberra complex. As noted above, station pointing and frequency predicts at this complex will be based on the pre-launch nominal trajectories derived from injection states supplied by the launch services provider, ULA. For most MSL launch opportunities, the second DSN complex to be able to track will be Madrid, approximately 4 to 8 hours after separation, and a predicts update will be required to have a high confidence that the acquisition at Madrid will be successful. The trajectory for updating the Madrid predicts will be generated by the MSL project navigation team using radio metric data from the DSN Canberra antennas, which will track the spacecraft prior to Madrid.

The effects of injection errors on the initial acquisition at the DSN stations are assessed using the injection covariance matrices (ICM) supplied by ULA. One particular aspect that was analyzed was the effect of the delay in transitioning to two-way Doppler on the accuracy of the orbit determination that will be used to point at the second DSN complex. Figure 6 shows the predicted pointing accuracy at the second DSN complex (Madrid's DSS 54) as a function of the delay in going two-way at the first DSN station (Canberra's DSS 34). Several cases are analyzed, varying the injection accuracy from its nominal value to higher values that would represent anomalous injections, and considering also the effect of removing or not the Doppler bias and signature produced by the spin of the spacecraft. The case selected for the study was the launch case with the shortest time between the first and second DSN complex rise. In the case of a nominal injection, removing the spin bias and signature in the Doppler is not required if the two-way Doppler can be acquired earlier than two and a half hours after the beginning of the pass. Going two-way earlier, or de-spinning the data, helps to improve the accuracy in the case of a degraded injection. The current plan is to transition to two-way not later than one hour after first signal acquisition, providing time for transmission and evaluation of the early spacecraft telemetry, and to be ready to de-spin the data, even for the first pass after launch.
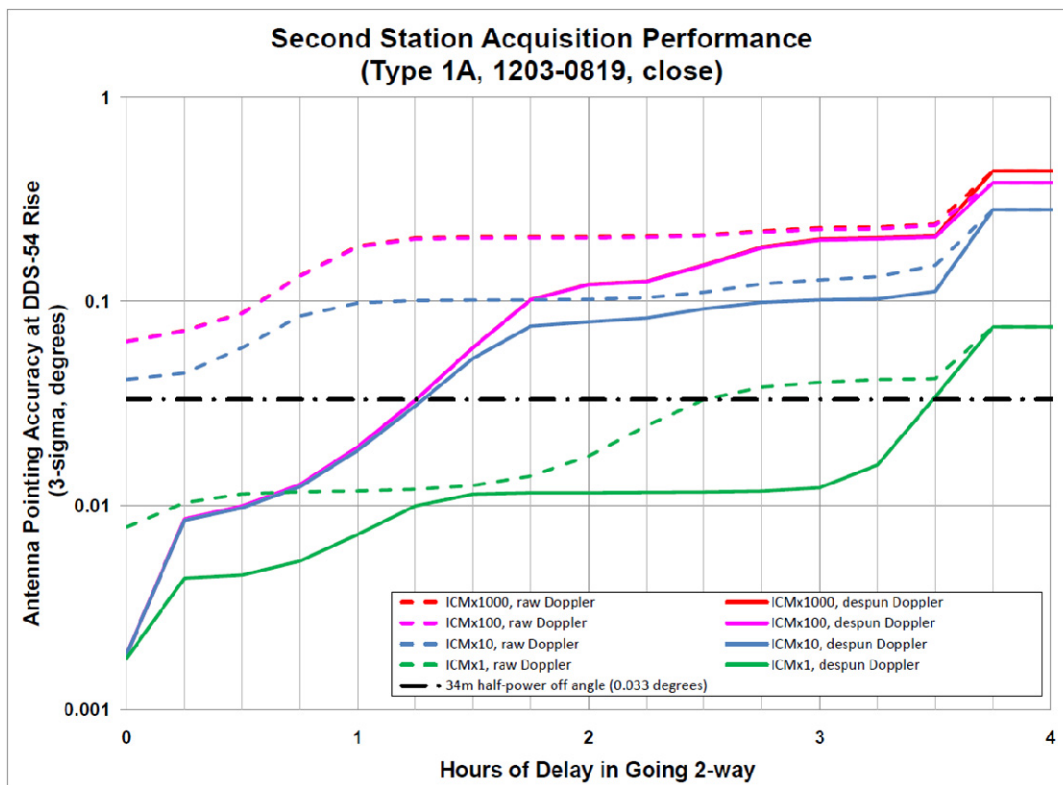
Figure 6. Effect of the Delay in going Two-way on Second Station Acquisition Performance

4. Cruise Phase

4.1. Trajectory Correction Maneuvers

Since the selection of the final landing site will not be known until after the final target specification is delivered to ULA, the MSL spacecraft will be targeted to a central landing site that reduces the cost of retargeting to any of the four candidate landing sites. Furthermore, the spacecraft cannot be directly targeted to enter Mars, since this will violate planetary protection requirements for the spacecraft and the upper stage. The spacecraft injection target needs to be biased away from Mars in order to reduce the probability of impact with Mars to below a prescribed level. A total of six TCMs are planned to remove injection errors and planetary protection bias, and to retarget from the central landing point to the actual landing site.

The TCMs will be performed using the cruise propulsion system, which consists of two clusters of four thrusters each located on opposite sides of the cruise stage. Each cluster has four thrusters at a 40 degree angle from a direction perpendicular to the spin axis, with a thruster oriented towards the spin axis, a thruster oriented away from the spin axis, and two normal to the spin axis, one towards the clockwise direction, and another towards the anti-clockwise direction. The center of mass of the spacecraft is offset with respect to the line joining the two thrusters. In order to use the thrusters without imparting a net torque to spacecraft, two possible firing modes are planned. In the axial mode two thrusters, the ones in each cluster most closely aligned with the desired axial direction, will fire simultaneously. In the lateral mode, all four thrusters in one cluster will fire for a given fraction of the spin period, with one thruster modulated to compensate for the center of mass offset. The same thrusters will be used for attitude control maneuvers, using different sets of thrusters for spin rate control and for turns.

The first three TCMs will be jointly optimized to reduce propellant consumption and fulfill planetary protection requirements, with TCM-3 being the first TCM that is targeted to the final entry interface point. TCM-4 and TCM-5 will be used to improve the delivery accuracy at the entry interface, while TCM-6 is a contingency maneuver opportunity that is not needed to achieve the required entry interface accuracy, but is available to correct an unplanned late anomaly. The first maneuver, TCM-1, will be performed while it is still possible to communicate using the PLGA, so this TCM can include turns to minimize propellant consumption. The other maneuvers will be performed while using the MGA, and the spacecraft will need to maintain its spin axis pointed towards the Earth while performing the maneuver, so those TCMs will be performed in vector mode, with a combination of axial and lateral burns.

4.2. Cruise Propellant Analysis

The total cruise propellant needed to deliver the spacecraft to the Mars entry interface point is the sum of the propellant used by the ACS system and the propellant used to execute TCMs. The total propellant consumption, for a given confidence level (typically 99%), needs to be below the total propellant loaded in the tanks in order to ensure a successful mission. The TCM propellant calculation accounts for initial injection dispersion, orbit determination covariance at each of the maneuver data cut-offs (DCO), expected maneuver implementation constraints and modes, and maneuver execution errors. Table 2 shows an example of statistical results for a particular launch/arrival case. The ideal ΔV is the total inertial velocity needed for each maneuver, including execution errors. The implemented ΔV takes into account the maneuver mode, thruster cant angle losses, and finite burn arc losses for lateral maneuvers, and the propellant mass includes the effects of the effective I_{sp} (accounting for plume impingement effects) for the maneuver mode used. Similar statistical propellant cost analyses have been performed for all launch/arrival cases, including the effect of variation of launch time within the daily launch window. The results confirm that the allocated 70 kg of cruise propellant will be sufficient for all the cases studied, with total required propellant at the 99% probability level being between approximately 38 and 52 kg [4].

Table 2. Deterministic, Ideal, and Implemented ΔV, and Propellant Mass Statistics – Type 1A Open, Mawrth

Type 1A Open 1125-0806-M (TCM-1/2/3 Opt. w/ PP constraints)

TCM	Location	Det. ΔV (m/s)	Ideal ΔV (m/s)			Implemented ΔV (m/s)			Propellant Mass (kg)		
			μ	1σ	ΔV_{99}	μ	1σ	ΔV_{99}	μ	1σ	ΔM_{99}
TCM-1	L + 15 d	0.97	2.39	1.65	7.28	3.62	2.58	11.29	6.86	4.96	21.58
TCM-2	L + 120 d	2.94	2.74	0.31	3.76	4.64	0.63	6.43	8.49	1.17	11.81
TCM-3	E - 60 d		0.38	0.10	0.62	0.68	0.19	1.17	1.25	0.35	2.17
TCM-4	E - 8 d		0.09	0.04	0.22	0.18	0.09	0.44	0.33	0.16	0.81
TCM-5	E - 2 d		0.02	0.01	0.04	0.03	0.02	0.08	0.06	0.03	0.15
Total		**3.91**	**5.63**	**1.53**	**10.39**	**9.15**	**2.45**	**16.90**	**16.99**	**4.71**	**31.82**

Assumptions and constraints:
- ICM from Feb 2010.
- Includes planetary protection biasing for injection, TCM-1 & TCM-2.
- TCM-1: MarsVZ mode; TCMs 2-5: vector mode.
- TCM-1 turn constraints: 75.0 deg off-Earth, 67.0 deg off-Sun.

- Injected mass = 4050 kg.
- Thruster cant angles = 50 deg (axial), 40 deg (lateral).
- Thrust per thruster = 3.0 N.
- Isp = 215.6 s (axial), 227.1 s (lateral).
- Angle between axial and lateral burn directions = 100.6 deg.
- Lateral burn arc = 5 s.

99% TCM propellant, kg	=	31.8
ACS propellant, kg	=	14.5
Total propellant, kg	=	46.3
Mission propellant allocation, kg	=	70.0
Propellant margin, kg	=	23.7 (34%)

4.3. ACS/NAV Calibration

One important activity that will be carried out during early cruise is the ACS/NAV calibration. The objective of the ACS/NAV calibration is to characterize the residual translational ΔV produced by spacecraft turns. A spacecraft turn uses pairs of thrusters firing in opposite directions, so it nominally produces zero net ΔV, but because the thrusters in general are not perfectly balanced, a small net ΔV will be produced. The residual ΔV for ACS turns plays a role in the propagation of the covariance for orbit predictions, since every one to two weeks a turn will be needed during late cruise and approach in order to maintain the PLGA antenna pointed towards the Earth. In the orbit determination baseline, a conservative estimate of the residual ΔV error is used for the covariance propagation. Therefore, characterizing the residual ΔV will lead to a more accurate, and hopefully smaller, orbit prediction covariance.

The ACS/NAV calibration consists of two identical sets of four small turns that are representative of the turns to be performed during late cruise and approach. During these turns, 2-way Doppler data are collected and used as observations to measure the net ΔV in the line of sight. The spacecraft attitude for each turn has been selected such that a complete reconstruction of the ACS residual ΔV vector is possible, taking into account that Doppler data only provide a measurement of the ΔV component along the line of sight. The spacecraft will first turn so that the angular momentum vector is at an angle of 45 deg away from the Earth. The first set of small turns will start with a turn away from the Earth's direction, then a turn normal to the Earth's direction, then the turn opposite to the last one, and then a turn towards the Earth. These four turns provide information on all three components of the net ΔV. The second set of turns is the same as the first set, and provides information on how repeatable the turn ΔV is.

After the execution of the ACS/NAV calibration, spacecraft telemetry will be collected and used to determine thruster firing times and the attitude of the spacecraft after each turn. Between each turn, Doppler data will be collected to allow for spin signature removal and to estimate the line-of-sight Doppler shift with sufficient accuracy. The three components of the net ΔV for each turn will be simultaneously estimated by the orbit determination filter. A mean value of the net ΔV will be calculated, along with the observed variability of the net turn ΔV from turn to turn.

5. Approach Phase

During the approach phase the main emphasis will be to produce a highly accurate orbit determination in order to predict the future trajectory of the spacecraft and to be able to design the TCMs needed to deliver the spacecraft to the desired atmospheric entry point.

5.1 Approach Covariance Analysis

In order to evaluate the accuracy with which the orbit determination will be performed, two sets of assumptions are used. The baseline set of assumptions uses conservative performance assumptions for all the inputs used by navigation, usually the required performance. The no-margin set of assumptions uses the expected performance, that is usually well below the published requirements. Table 3 shows the baseline assumptions used for the MSL Final Navigation Plan, while Table 4 shows the no-margin assumptions, with the changes with respect to the baseline highlighted.

The approach covariance analysis is based on a data arc starting 60 days before entry, and uses the DSN tracking schedule that has been planned for operations. During the approach phase the DSN will perform five tracking passes per week up to entry minus 45 days, and continuous tracking afterwards. Delta Differenced One-way Range (ΔDOR) measurements will be performed twice per

week up to 28 days before entry and twice per day afterwards, using alternating Goldstone-Canberra and Goldstone-Madrid baselines. ESA DΔDOR data, using the Cebreros-New Norcia baseline, will also be collected daily for the 14 days before entry, but it is considered a backup for a missing DSN baseline and it is not used in the baseline assumptions.

Table 3. Main Baseline Covariance Assumptions

Error Source	Estimate or Consider	A Priori Uncertainty (1σ)	Correlation Time	Update Time	Reasoning/Comments
Epoch state position (km)	Est.	1000	–	–	
Epoch state velocity (km/s)	Est.	1	–	–	
X-Band 2-way Doppler (mm/s)	–	0.1	–	–	5.62 mHz, MER performance
Range (m)	–	3	–	–	21.03 RU, low SNR during late cruise
ΔDOR (ps)	–	60	–	–	~2.4 nrad
Doppler Bias (mm/s)	Est.	0.002	0	Per pass	Residual error from spin bias estimation
Range Bias (m)	Est.	2	0	Per pass	DSN performance
Station Locations (cm)	Con.	Full 2003 cov.	–	–	
Quasar Locations (nrad)	Con.	1	–	–	
Pole X, Y (cm)	Est	1 - 4	48 hrs	6 hrs	Slope 2 days before EOP to EOP+12h.
UT1 (cm)	Est	1.7 - 15	48 hrs	6 hrs	Slope 6 days before EOP to EOP+12h.
Ionosphere–day/night (cm)	Est	55/15	6 hrs	1 hr	S-band units; use 6x (iono) and 2x (trop) apsig when no actuals; subsequent passes uncorrelated.
Troposphere–wet/dry (cm)	Est	1/1	6 hrs	1 hr	
Mars and Earth Ephemerides	Con.	DE414 Covariance	–	–	
Mars GM (km^3/s^2)	Con.	2.80 x 10^{-4}	–	–	~10x MGS95J formal error
Solar Pressure					High-fidelity model.
Gr - radial component (%)	Est.	5	7 days	1 day	Correlation broken at turns. Gr and Gx estimated as both a bias and stochastic.
Gx - tangential component (%)	Est.	5	7 days	1 day	
Gy - out of plane component (%)	Est.	1	–	–	
Non-gravitational Accelerations (km/s^2)	–	0	–	–	Accommodated in SRP model.
ACS Event ΔV (mm/s)	First turn at L+15 days, then every 7 days until E-8 days				Conservative assumption
Per Axis	Est.	2 mm/s before E-45d 1 mm/s after E-45d	–	–	Flight system requirement.
Maneuver Execution Errors (mm/s)					Range of values for current set of cases.
TCM 4 (E-8d)	Est.	2.34 - 2.84	–	–	5% proportional error and 4 mm/s fixed error (3σ), vector mode maneuver.
TCM 5 (E-2d)	Est.	1.91 - 1.93	–	–	

The expected errors in the Mars ephemeris, relative to the Earth and at the time of entry, are predicted to be less than 10 meters in line of sight, 125 meters in right ascension and 225 meters in declination. Regular ΔDOR measurements of MRO and Odyssey, currently in orbit around Mars, as well as range measurements, are being incorporated in the planetary ephemerides improvement process in order to reduce the future uncertainty of the ephemerides. The MSL project will receive its final ephemerides, with the most up-to-date measurements and models, three months before arrival to Mars.

Table 4. Main No-Margin Error Assumptions

Error Source	Estimate or Consider	A Priori Uncertainty (1σ)	Correlation Time	Update Time	Reasoning/Comments
Epoch state position (km)	Est.	1000	–	–	
Epoch state velocity (km/s)	Est.	1	–	–	
X-Band 2-way Doppler (mm/s)	–	0.05	–	–	2.81 mHz, MER performance
Range (m)	–	3	–	–	21.0305 RU, low SNR during late cruise
ΔDOR (ps)	–	40	–	–	~1.6 nrad – Expected performance on 70m and BWG with improved LNAs and newly-engineered microwave feed systems
Doppler Bias (mm/s)	-	-	-	-	Not needed when the spin rate estimation error is neglibly small
Range Bias (m)	Est.	1	0	Per pass	Expected DSN performance
Station Locations (cm)	Con.	Full 2003 cov.	–	–	
Quasar Locations (nrad)	Con.	1	–	–	
Pole X, Y (cm)	Est	1	48 hrs	6 hrs	No change from fit to predict.
UT1 (cm)	Est	1.7 – 7.5	48 hrs	6 hrs	Slope 6 days before EOP to EOP+12h.
Ionosphere–day/night (cm)	Est	55/15	6 hrs	1 hr	S-band units; use 6x (iono) and 2x (trop) apsig when no actuals; subsequent passes uncorrelated.
Troposphere–wet/dry (cm)	Est	1/1	6 hrs	1 hr	
Mars and Earth Ephemerides	Con.	0.5 x DE414 Covariance			Assumes improvement with additional 1/month ΔDOR to MRO and Odyssey
Mars GM (km³/s²)	Con.	2.80×10^{-4}	–	–	~10x MGS95J formal error
Solar Pressure					High-fidelity model.
Gr - radial component (%)	Est.	2	7 days	1 day	Correlation broken at turns. Gr, Gx estimated as both a bias and stochastic.
Gx - tangential component (%)	Est.	2	7 days	1 day	
Gy - out of plane component (%)	Est.	1	–	–	
Non-gravitational Accelerations (km/s²)	–	0	–	–	Accommodated in SRP model.
ACS Event ΔV (mm/s)	First turn at L+15 days, then every 7 days until E-8 days				Conservative assumption
Per Axis	Est.	0.1 mm/s for all turns	–	–	MER-B worst case performance
Maneuver Execution Errors (mm/s)					Range of values for current set of cases.
TCM 4 (E-8d)	Est.	1.68 – 2.32	–	–	5% proportional error and 2 mm/s fixed error (3σ), vector mode maneuver.
TCM 5 (E-2d)	Est.	0.99 – 1.03	–	–	

Entry delivery and knowledge accuracies have been computed using these baseline and no-margin assumptions. An example of these results is shown in Table 5. These calculations have been performed for all launch/arrival cases, and for all four landing sites. The rows of Table 5 are grouped as follows: case characteristics, TCM-4 delivery, TCM-5 delivery, entry knowledge without TCM-5, and entry knowledge with TCM-5. Entry knowledge uncertainties are provided for two different data cutoff epochs corresponding to the on-board entry state update opportunities at entry minus 33 hours and entry minus 6 hours. The highlighted rows in the tables indicate the parameters that have requirements levied against them: ±0.20 deg in entry flight path angle (EFPA) delivery, 2.8 km in position knowledge and 2.0 m/s in velocity knowledge, all 3σ. If a given value exceeds its requirement, the cell in the table is colored red. The results show that the baseline TCM-4 EFPA delivery accuracy does not meet the ±0.20 deg (3-sigma) requirement for all launch days

and landing sites; however, the requirement is met at TCM-5 and for the no-margin TCM-4 and TCM-5 delivery cases. The baseline and the no-margin entry minus 6 hour data cut-off entry knowledge accuracies (position and velocity) are below the requirement of 2.8 km and 2.0 m/sec, respectively, with the no-margin knowledge at entry minus 33 hours data cut-off being below the requirement for most cases.

Table 5. Baseline and No-Margin Results for Mawrth (M), Gale (G) and Holden (H) for Launch on November 25, 2011 and Arrival on August 6, 2012

Case	1125-0806-M		1125-0806-G		1125-0806-H	
Launch Date	25-NOV-2011		25-NOV-2011		25-NOV-2011	
Arrival Date	06-AUG-2012		06-AUG-2012		06-AUG-2012	
Landing Site Name	Mawrth Vallis		Gale Crater		Holden Crater Fan	
Epoch of the Data Arc	E-44.9 days		E-45.5 days		E-45.0 days	
Entry Flight Path Angle	- 15.50 deg		- 15.50 deg		- 15.50 deg	
Entry Flight Path Angle Requirement (3σ)	0.2 deg		0.2 deg		0.2 deg	
Entry Position Knowledge Requirement (3σ)	2.8 km		2.8 km		2.8 km	
Entry Velocity Knowledge Requirement (3σ)	2.0 m/sec		2.0 m/sec		2.0 m/sec	
B-plane Angle	- 26.25 deg		3.96 deg		27.20 deg	
dB/d(EFPA)	27.9 km/deg		27.9 km/deg		27.9 km/deg	
	Baseline	No-Margin	Baseline	No-Margin	Baseline	No-Margin
TCM-4 Delivery:						
Data Cutoff Epoch	E-8.4 days	E-8.4 days	E-9.0 days	E-9.0 days	E-8.5 days	E-8.5 days
Apriori TCM-4 Execution Error (3σ)	7.68 mm/sec	5.92 mm/sec	7.84 mm/sec	6.12 mm/sec	8.33 mm/sec	6.74 mm/sec
Semi-major Axis (3σ)	6.66 km	4.48 km	7.19 km	4.89 km	7.04 km	5.01 km
Semi-minor Axis (3σ)	6.12 km	4.34 km	6.62 km	4.77 km	6.55 km	4.91 km
Ellipse Orientation Angle	159.4 deg	156.7 deg	161.6 deg	160.8 deg	161.0 deg	161.5 deg
Linearized Flight Time (3σ)	1.62 sec	1.14 sec	1.75 sec	1.26 sec	1.74 sec	1.30 sec
Entry Time (3σ)	4.17 sec	2.87 sec	4.51 sec	3.16 sec	4.40 sec	3.26 sec
B Magnitude (3σ)	6.66 km	4.48 km	7.11 km	4.87 km	6.79 km	4.96 km
d($3\sigma_{EFPA}$)/d(EFPA)	0.015 deg/deg	0.010 deg/deg	0.016 deg/deg	0.011 deg/deg	0.015 deg/deg	0.011 deg/deg
Entry Flight Path Angle (3σ)	± 0.24 deg	± 0.16 deg	± 0.25 deg	± 0.17 deg	± 0.24 deg	± 0.18 deg
TCM-5 Delivery:						
Data Cutoff Epoch	E-2.5 days	E-2.5 days	E-2.5 days	E-2.5 days	E-2.5 days	E-2.5 days
Apriori TCM-5 Execution Error (3σ)	5.74 mm/sec	3.00 mm/sec	5.76 mm/sec	3.02 mm/sec	5.76 mm/sec	3.02 mm/sec
Semi-major Axis (3σ)	2.97 km	1.79 km	3.10 km	1.72 km	3.01 km	1.81 km
Semi-minor Axis (3σ)	2.20 km	1.35 km	2.27 km	1.30 km	2.22 km	1.37 km
Ellipse Orientation Angle	149.4 deg	137.3 deg	149.0 deg	147.9 deg	149.3 deg	136.4 deg
Linearized Flight Time (3σ)	0.49 sec	0.29 sec	0.50 sec	0.27 sec	0.50 sec	0.29 sec
Entry Time (3σ)	1.51 sec	0.86 sec	1.51 sec	0.83 sec	1.42 sec	0.83 sec
B Magnitude (3σ)	2.97 km	1.76 km	2.86 km	1.58 km	2.47 km	1.42 km
d($3\sigma_{EFPA}$)/d(EFPA)	0.007 deg/deg	0.004 deg/deg	0.006 deg/deg	0.004 deg/deg	0.006 deg/deg	0.003 deg/deg
Entry Flight Path Angle (3σ)	± 0.11 deg	± 0.06 deg	± 0.10 deg	± 0.06 deg	± 0.09 deg	± 0.05 deg
Entry Knowledge Without TCM-5 (3σ)						
Position @ E-33h	2.32 km	1.44 km	2.63 km	1.67 km	2.80 km	1.82 km
Velocity @ E-33h	1.32 m/sec	0.82 m/sec	1.56 m/sec	1.01 m/sec	1.71 m/sec	1.13 m/sec
Position @ E-6h	1.16 km	0.81 km	1.58 km	1.08 km	1.79 km	1.22 km
Velocity @ E-6h	0.78 m/sec	0.54 m/sec	1.08 m/sec	0.74 m/sec	1.23 m/sec	0.84 m/sec
Entry Knowledge With TCM-5 (3σ)						
Position @ E-33h	2.49 km	1.54 km	2.82 km	1.78 km	3.04 km	1.94 km
Velocity @ E-33h	1.41 m/sec	0.88 m/sec	1.68 m/sec	1.07 m/sec	1.87 m/sec	1.20 m/sec
Position @ E-6h	1.24 km	0.84 km	1.67 km	1.11 km	1.90 km	1.26 km
Velocity @ E-6h	0.83 m/sec	0.56 m/sec	1.14 m/sec	0.76 m/sec	1.31 m/sec	0.86 m/sec

5.2 Approach Sensitivity Analysis

A series of parameterized sensitivity studies for the approach phase were performed in order to determine the effects of changes to data assumptions and modeling uncertainties on the TCM-4 and TCM-5 delivery accuracies and the entry knowledge accuracies. For all cases studied, only a single parameter or model is changed with respect to the baseline. The changes in the error sources are summarized in Table 6. For comparison purposes, the table includes the applicable baseline and no-margin assumptions. In general, the improved case uses half the baseline value for a given parameter, whereas the degraded case uses twice the baseline value. Other permutations evaluated include different tracking data combinations with the baseline assumptions. The baseline case includes all tracking data types: Doppler, range and ΔDOR. Variations include the following: Doppler, range and North-South (N-S) ΔDOR; Doppler, range and East-West (E-W) ΔDOR; Doppler and range; Doppler and ΔDOR; and Doppler only. Furthermore, the following three cases with ESA ΔDOR data were included: using only ESA ΔDOR data, use ESA ΔDOR data and omit Madrid data or use ESA ΔDOR data and omit Canberra data, and also a case using Emergency Control Center (ECC) assumptions. The Emergency Control Center will be operational for the last few days before entry, and it will be used if the facilities at JPL cannot be used to perform the

navigation function. In that case, it is assumed that ΔDOR data, media corrections and Earth orientation parameter updates will not be available.

Table 6. Error Assumptions For Sensitivity Analyses

Error Source	Estimate or Consider	Uncertainties (1σ)			
		Improved	Baseline	Degraded	No Margin
2-way Doppler weight (mm/s)	-	0.05	0.1	0.2	0.05
Range weight (m)	-	1.5	3	6	3
ΔDOR weight (ps)	-	30	60	120	40
ΔDOR latency (hr)	-	12	24	48	8
ACS Turns (per axis, mm/s)	Est	0.5 x Baseline	2 or 1	2 x Baseline	0.1
TCM-4 (per axis, mm/s)*	Est	0.5 x Baseline	5% Prop + 4 mm/s Fixed	2 x Baseline	5% Prop + 2 mm/s Fixed
TCM-5 (per axis, mm/s)*	Est	0.5 x Baseline	5% Prop + 4 mm/s Fixed	2 x Baseline	5% Prop + 2 mm/s Fixed
Solar Pressure: GR, GX, GY (%)	Est	2.5, 2.5, 1	5, 5, 1	10, 10, 1	2, 2, 1
Mismodeled Solar Pressure: GR, GX (%)	Est (stoch)	2.5, 2.5	5, 5	10, 10	2, 2
Doppler Bias (mm/s)	Est (stoch)	0.001	0.002	0.004	0
Range Bias (m)	Est (stoch)	1	2	4	1
Day Ionosphere (S-Band, cm)	Est (stoch)	27.5	55	110	55
Night Ionosphere (S-Band, cm)	Est (stoch)	7.5	15	30	15
Wet Troposphere (cm)	Est (stoch)	0.5	1	2	1
Dry Troposphere (cm)	Est (stoch)	0.5	1	2	1
X/Y Pole, recon. --> predict (cm)	Est (stoch)	1 to 2	1 to 4	1 to 8	1
UT1, recon. --> predict (cm)	Est (stoch)	1.7 to 7.5	1.7 to 15	1.7 to 30	1.7 to 7.5
Quasar Locations (nrad)	Con	0.5	1	2	1
Earth-Mars Ephemeris	Con	0.5 x Cov	1.0 x Cov	2.0 x Cov	0.5 x Cov

Figures 7 and 8 are examples, as bar charts, of sensitivity results. The charts list the individual cases along the bottom, beginning with the baseline (green) and no-margin (yellow) cases, followed by the variations of error assumptions and data weights (blue for improved, red for degraded), followed by tracking data combinations (orange). For comparison, a red dashed horizontal line indicates the requirement level, and a green dotted horizontal line indicates the Baseline level. The vertical axis limit is set to twice the requirement level; the bars that extend past that level have their value listed in the top of the bar.

Figure 7 shows the EFPA delivery sensitivities with TCM-5 for Type 1A open targeted to Gale. Inspection of this and other similar plots for other cases and for TCM-4 reveals that the most significant sensitivities for TCM-4 delivery are TCM execution error and ACS turn ΔV, and for TCM-5 delivery, they are TCM execution error, SRP stochastic errors, and ΔDOR parameters (weight, latency and quasar position). The data type variations show that the solution is most sensitive to ΔDOR weight and loss of ΔDOR measurements. Figure 8 shows the entry position knowledge sensitivities at the entry minus 6 hour DCO for the same case. This and other similar plots for other cases and for velocity knowledge reveal that the most significant entry knowledge sensitivities are ΔDOR weight, planetary ephemeris, TCMs, and quasar positions. The plots also show that the navigation performed from the ECC can fulfill requirements in most cases using the baseline assumptions; and will fulfill them using no-margin assumptions, and that the ESA ΔDOR provides an adequate backup for the case in which a DSN ΔDOR baseline is not available.
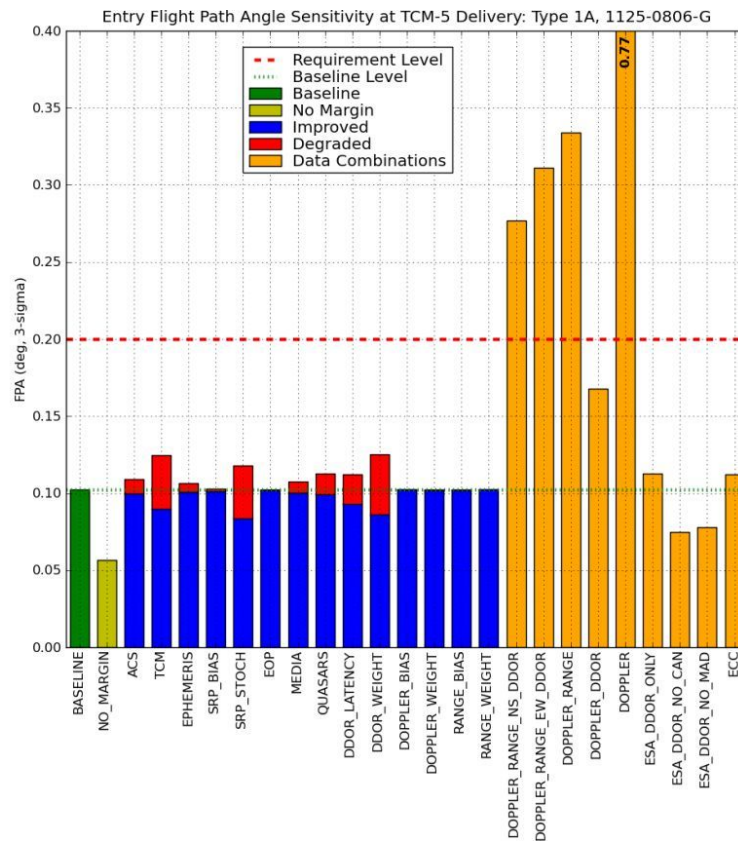
Figure 7. Example of Entry Flight Path Angle Sensitivity Analysis for a TCM-5 Delivery
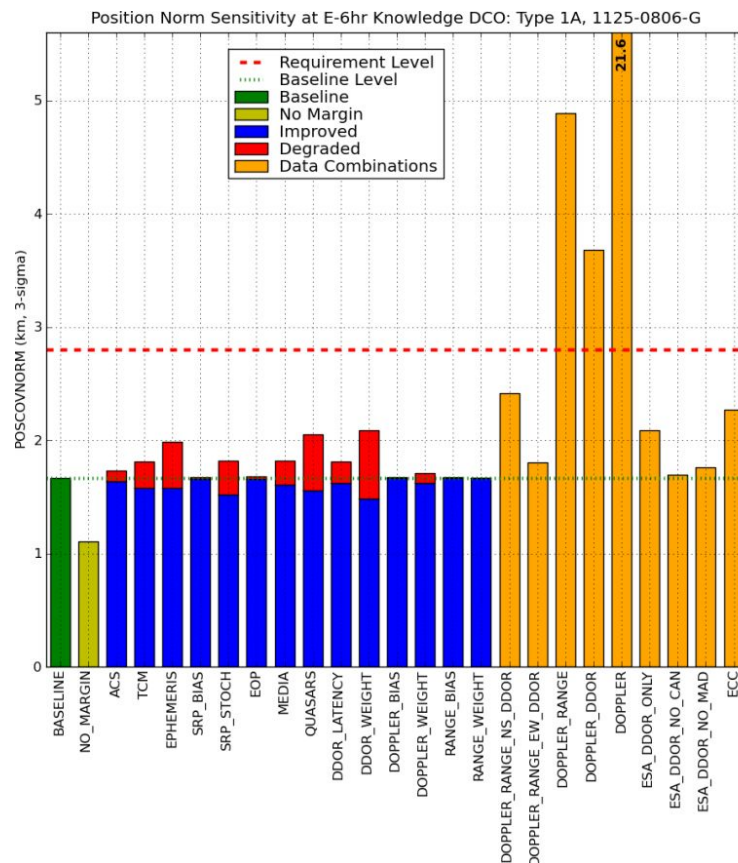

**Figure 8. Example of Position Knowledge Sensitivity Analysis for an Entry minus 6 Hours
Data Cut-off**

6. EDL Monitoring

The navigation system is required to acquire and process DTE Doppler data for real-time monitoring of TCMs and EDL. Streaming, two-way, coherent Doppler will be used to observe TCMs-5, 5X and 6. Minutes before cruise stage separation, and in order to transmit MFSK tones, the telecom system will be switched to a non-coherent mode. During the final approach phase, streaming one-way, non-coherent Doppler will be used to observe, to the maximum extent possible in real-time, EDL-related events from the Heat Rejection System (HRS) venting through parachute deployment. If the DSN loses lock on the signal, real-time detection will not be possible; however, the open-loop recording process should store the necessary data for later analysis, as long as the signal path is not occulted by Mars.

7. Conclusion

Pre-launch analysis has shown that the MSL navigation system will be able to fulfill the demanding requirements levied on it to successfully land the MSL rover on the surface of Mars.

8. Acknowledgments

Reference herein to any specific commercial product, process, or service by trade name, trademark, manufacturer, or otherwise, does not constitute or imply its endorsement by the United States Government or the Jet Propulsion Laboratory, California Institute of Technology.

9. References

[1] Mars Exploration Program Landing Sites, http://marsoweb.nas.nasa.gov/landingsites.

[2] Grant, J., "Intro to Workshop and Process", Fourth MSL Landing Site Workshop, September 27, 2010.

[3] Mars Science Laboratory Mission Fact Sheet, http://mars.jpl.nasa.gov/msl/news/pdfs/MSL-200608.pdf.

[4] MSL 2011 Final Navigation Plan, JPL D-33445, September 1, 2010.